

# Relative Proton Affinities from Kinetic Energy Release Distributions for Dissociation of Proton-Bound Dimers

John J. Hache, Julia Laskin,\* and Jean H. Futrell

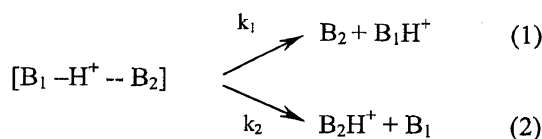
Pacific Northwest National Laboratory, William R. Wiley Environmental Molecular Sciences Laboratory, P. O. Box 999 (K8-96), Richland, Washington 99352

Received: July 12, 2002; In Final Form: September 6, 2002

Kinetic energy release distributions (KERDs) upon dissociation of proton-bound dimers are utilized along with finite heat bath theory analysis to obtain relative proton affinities of monomeric species composing the dimer. The proposed approach allows accurate measurement of relative proton affinities based on KERD measurements for the compound with unknown thermochemical properties vs a single reference base. It also allows distinguishing the cases when dissociation of proton-bound dimers is associated with a reverse activation barrier, for which both our approach and the kinetic method become inapplicable. Results are reported for the *n*-butanol–*n*-propanol dimer, for which there is no significant difference in entropy effects for two reactions, and for the pyrrolidine–1,2-ethylenediamine dimer, which is characterized by a significant difference in entropy effects for the two competing reactions. Relative protonation affinities of  $-1.0 \pm 0.3$  kcal/mol for the *n*-butanol–*n*-propanol pair and  $0.27 \pm 0.10$  kcal/mol for the pyrrolidine–1,2-ethylenediamine pair are in good agreement with literature values. Relative reaction entropies were extracted from the branching ratio and KERD measurements. Good correspondence was found between the relative reaction entropies for the *n*-butanol–*n*-propanol dimer ( $\Delta(\Delta S^\ddagger) = -0.3 \pm 1.5$  cal/mol K) and the relative protonation entropy for the two monomers ( $\Delta(\Delta S_p) = 0$ ). However, the relative reaction entropy for the pyrrolidine–1,2-ethylenediamine dimer is higher than the difference in protonation entropies ( $\Delta(\Delta S^\ddagger) = 8.2 \pm 0.5$  cal/mol K vs  $\Delta(\Delta S_p) = 5$  cal/mol K).

## Introduction

Dissociation of proton-bound dimers following reactions 1 and 2 has been widely utilized for determination of the relative proton affinity and the gas phase basicity of a compound with unknown thermochemical properties ( $B_1$ ) relative to a reference base  $B_2$  with known proton affinity: The kinetic method for



thermochemical determinations introduced by Cooks and co-workers<sup>1,2</sup> assumes that the two monomers composing the dimer compete for the proton based on their relative proton affinities. In the simplest case, when the entropy effects for two reactions 1a,b are the same and both reactions have a negligible reverse activation barrier, the experimentally measured branching ratio is given by a simple expression:

$$\ln\left(\frac{k_1}{k_2}\right) = \frac{PA(B_1) - PA(B_2)}{RT_{\text{eff}}} \quad (3)$$

where  $PA(B_1)$  and  $PA(B_2)$  are proton affinities of  $B_1$  and  $B_2$ , respectively, and  $T_{\text{eff}}$  is the effective temperature. Measuring the branching ratio of the two monomers for several reference bases and plotting it as a function of the proton affinity of the reference base ( $PA(B_2)$ ) gives a straight line with the slope given

by  $-1/RT_{\text{eff}}$  and the intercept of  $PA(B_1)/RT_{\text{eff}}$ . The proton affinity of  $B_1$  is then derived from the slope and the intercept of the kinetic plot. We have recently analyzed the kinetic method formalism using finite heat bath theory (FHBT)<sup>4,5</sup> and concluded that the effective temperature can be identified with the average transition state temperature for reaction 2,<sup>5</sup> a measure of the excess internal energy above the dissociation threshold for the reaction.

When the entropy effects of the two reactions are different, the branching ratio depends on the entropy difference  $\Delta(\Delta S^\ddagger) = \Delta S_2^\ddagger - \Delta S_1^\ddagger$  in the following way:

$$\ln\left(\frac{k_1}{k_2}\right) = \frac{PA(B_1) - PA(B_2)}{RT_{\text{eff}}} - \frac{\Delta(\Delta S^\ddagger)}{R} \quad (4)$$

Equation 4 has been utilized in the extended version of the kinetic method developed by Fenselau and co-workers.<sup>6</sup> In this method, the branching ratios are measured at different collision energies, corresponding to different effective temperatures. The effective temperatures are extracted from the slopes of the kinetic plots. The unknown proton affinity and the entropy difference,  $\Delta(\Delta S^\ddagger)$ , are determined from the temperature-dependent intercepts (intercept =  $PA(B_1)/RT_{\text{eff}} - \Delta(\Delta S^\ddagger)/R$ ). This approach assumes that  $\Delta(\Delta S^\ddagger)$  is the same for all reference bases and therefore requires a choice of bases that are structurally similar among themselves but not necessarily similar to the unknown ( $B_1$ ).

Unfortunately, experimental branching ratios are very sensitive to small changes in the gas phase basicity of the reference base, and in many cases, it is difficult to find a set of structurally

\* To whom correspondence should be addressed. Fax: (509)376-3650. E-mail: Julia.Laskin@pnl.gov.

similar bases with known proton affinity to map the proton affinity of the unknown. For this reason, Cooks and co-workers introduced an entropy-corrected version of the kinetic method,<sup>7</sup> in which the entropy term in eq 4 is explicitly rewritten as  $\Delta(\Delta S^\ddagger)/R = \Delta S_2^\ddagger/R - \Delta S_1^\ddagger/R$  and the equation is rearranged to yield

$$\ln\left(\frac{k_1}{k_2}\right) + \frac{\Delta S_2^\ddagger}{R} = \frac{\text{PA}(\text{B}_1) - \text{PA}(\text{B}_2)}{RT_{\text{eff}}} + \frac{\Delta S_1^\ddagger}{R} \quad (5)$$

The branching ratio for each pair of compounds is corrected by the entropy term of the reference base. The unknown proton affinity and entropy change of reaction 1a are then determined using the same procedure described above. This approach can be utilized for thermochemical determination using a set of structurally dissimilar reference bases. However, it requires knowledge of the entropy effect associated with reaction 2 ( $\Delta S_2^\ddagger$ ), which was assumed to be equal to the protonation entropy of the reference base ( $\text{B}_2$ ).<sup>7</sup>

In this work, we test the different approach proposed in our previous study<sup>5</sup> that relies on rate equations derived using FHBT. We have shown that the branching ratio for two reactions can be expressed as<sup>5</sup>

$$\ln\left(\frac{k_1}{k_2}\right) = \frac{\Delta(\Delta S^\ddagger)}{k_B} + C \ln\left(\frac{T_1^\ddagger}{T_2^\ddagger}\right) \quad (6)$$

where  $C$  is the heat capacity of the energized ion, while  $T_1^\ddagger$  and  $T_2^\ddagger$  are the transition state temperatures for reactions 1 and 2, respectively. The difference in threshold energies for reactions 1 and 2 is given by

$$\Delta E_2 - \Delta E_1 = \bar{E}_1^\ddagger(T_1^\ddagger) - \bar{E}_2^\ddagger(T_2^\ddagger) \quad (7)$$

where  $\bar{E}^\ddagger(T^\ddagger)$  is the average energy of the transition state evaluated at temperature  $T^\ddagger$ . If reactions 1 and 2 have negligible reverse activation barriers, the relative proton affinity is then obtained from eq 8:

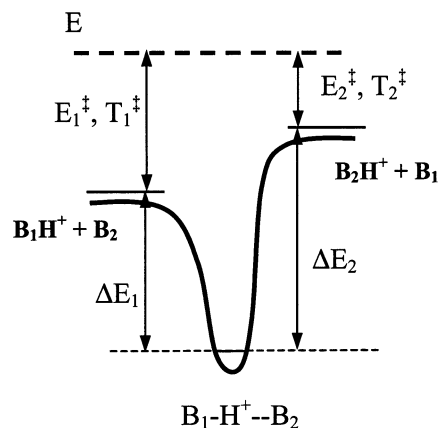
$$\text{PA}(\text{B}_1) - \text{PA}(\text{B}_2) = \Delta H_2 - \Delta H_1 = \Delta E_2 - \Delta E_1 \quad (8)$$

The final essential point of our proposed method is that transition state temperatures for both reaction channels can be derived from kinetic energy release (KER) measurements. Various aspects of obtaining kinetic energy release distributions (KERDs) from metastable peak measurements and theoretical approaches for extracting thermochemical information from KERDs have been recently reviewed.<sup>8</sup> One of the simplest parametric approaches introduced by Klots<sup>9</sup> and extensively utilized in studies on cluster ion dissociation<sup>10,11</sup> represents the KERD for reactions with no reverse activation barrier in the following form:

$$P(\epsilon) = \epsilon^l \exp(-\epsilon/k_B T^\ddagger) \quad (9)$$

where  $l$  is a parameter ( $0 < l < 1$ );  $T^\ddagger$  is the transition state temperature for reaction; and  $k_B$  is Boltzmann's constant. The average KER is given by  $(l + 1)k_B T^\ddagger$ . Fitting the experimental KERD with the above function yields the transition state temperature for the reaction.

The expected trends in experimentally measured KERs and corresponding transition state temperatures for dissociation of a proton-bound dimer  $\text{B}_1\text{-H}^+ \text{-B}_2$  with internal energy  $E$  can be predicted by examining the hypothetical potential energy



**Figure 1.** Schematic drawing of the potential energy surface for dissociation of a proton-bound dimer  $[\text{B}_1\text{-H}^+ \text{-B}_2]$  via reactions 1 and 2.

surface illustrated in Figure 1. In this case, the proton affinity of  $\text{B}_1$  is higher than the proton affinity of the reference base and the threshold energy for reaction 1 ( $\Delta E_1$ ) is lower than the threshold energy for reaction 2 ( $\Delta E_2$ ). Consequently, reaction 1 is characterized by higher excess internal energy ( $E_1^\ddagger$ ), higher transition state temperature ( $T_1^\ddagger$ ), and larger KER, i.e., the higher proton affinity is associated with larger experimental KER. The entropy difference for the two reactions will be reflected in the branching ratio (eq 6).

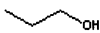
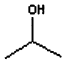

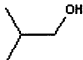
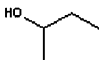


These principles are combined in the proposed approach, which relies on measurement of both the branching ratio for reactions 1 and 2 and the metastable peak shapes for the two ionic fragments. It is remarkable that both the relative proton affinity and the difference in reaction entropies can be obtained from a kinetic measurement of the compound with unknown thermochemical properties using a single reference base. Moreover, structural similarity between the two monomers is not required, allowing for a very flexible choice of the reference base. This represents the most general approach for deducing the relative energetics and dynamics for competing reactions using the kinetic method, provided reactions 1 and 2 have negligible reverse activation barriers.

## Experimental Section

**Mass Spectrometry.** Experiments were performed on a triple sector (EBE) Micromass ZabSpec (ZS017) mass spectrometer modified for accurate measurement of KERDs. The instrument modification involved incorporation of two beam-limiting apertures (0.4 mm) at the beginning and the end of the second field free region in order to restrict the measurement of KERDs to ions dissociating along the  $z$ -axis (parallel to the ion beam).<sup>12–14</sup> KERD measurements were calibrated by monitoring metastable peak shapes for the loss of hydrogen and  $\text{C}_2\text{H}_2$  from  $\text{C}_6\text{H}_6^{+*}$ , for which accurate KER values have been established.<sup>15</sup> Mass-analyzed ion kinetic energy spectra (MIKEs) were obtained by scanning the second electric sector.

Proton-bound dimers were generated in a CI source by self-protonation. The ion source conditions were as follows: source temperature, 100 °C; filament emission current, 0.6–1.1 mA; electron energy, 20–50 eV; pressure,  $(4\text{--}6) \times 10^{-5}$  Torr, as monitored by the ionization gauge; acceleration voltage, 6 kV. The temperature of the liquid inlet system was optimized for the efficient formation of proton-bound dimers. All chemicals were purchased from Aldrich and used as received. *iso*-Propyl-1,1,1,3,3,3-*d*6 alcohol,  $(\text{CD}_3)_2\text{CHOH}$ , was purchased from CDN Isotopes (Quebec, Canada).

TABLE 1: Structures and Thermochemical Properties of Model Systems used in this Study (ref 20)

Molecule	Structure	GB, kcal/mol	PA, kcal/mol	S <sub>p</sub> , cal/mol K
n-Propanol		180.7	188.0	1.7
2-Propanol		182.3	189.5	1.7
n-Butanol		181.4	188.6 <sup>a</sup>	1.7
Isobutanol		182.2	189.7	0.7
2-Butanol		187.5	194.8	1.7
1,2-Ethylenediamine		218.1	227.4	-5.3
Pyrrolidine		218.8	226.6	-0.3

<sup>a</sup> Holmes et al.<sup>19</sup> suggested adjusting the PA of *n*-butanol to 189.7 kcal/mol.

Experimental metastable peaks were smoothed using a piecewise cubic spline smoothing routine. KERDs were obtained by differentiating the smoothed metastable peaks and converting the kinetic energy from the laboratory into the center-of-mass frame using a standard expression.<sup>8</sup>

**Modeling.** Experimental KERDs were fitted with the two parameter function given in eq 9 to yield transition state temperatures for reactions 1 and 2. The difference in reaction entropies,  $\Delta(\Delta S^\ddagger)$ , was calculated from the experimental branching ratio and the two transition state temperatures using eq 6. The difference in the dissociation thresholds was obtained using eq 7. The average energy in eq 7 and the heat capacity in eq 6 were calculated using standard expressions:

$$\langle E \rangle = \sum_{i=1}^N \frac{h\nu_i}{\exp(h\nu_i/k_B T) - 1} \quad (10a)$$

$$C = \sum_{i=1}^N \frac{(h\nu_i/k_B T)^2 \exp(-h\nu_i/k_B T)}{[1 - \exp(-h\nu_i/k_B T)]^2} \quad (10b)$$

where  $\nu_i$  is the vibrational frequency,  $h$  is Plank's constant,  $k_B$  is Boltzmann's constant,  $T$  is the temperature, and  $c$  is the velocity of light. Vibrational frequencies of butanol–propanol dimers were estimated by propagating ab initio vibrational frequencies of smaller alcohol dimers given in ref 16. Vibrational frequencies of 1,2-ethylenediamine–pyrrolidine dimer were estimated by combining vibrational frequencies of neutral pyrrolidine<sup>17</sup> and protonated ethylenediamine<sup>18</sup> and assuming five more dimer common modes in the range of 100–300 cm<sup>-1</sup>. It should be noted that calculated results were not very sensitive to the values of vibrational frequencies. The uncertainties in the values of  $\Delta(\Delta S^\ddagger)$  and  $\Delta(\Delta E)$  related to the uncertainties in vibrational frequencies are much smaller than the experimental error bars that have been assigned to the dissociation energy and entropy differences.

## Results and Discussion

In this section, we will present two test cases for the approach proposed in the Introduction. Dissociation of proton-bound alcohol dimers is a good example of competing reactions without reverse activation barriers and with equivalent entropy (i.e.,  $\Delta(\Delta S^\ddagger) = 0$ ). The kinetic method has been successfully applied previously to the proton affinities of primary alcohols.<sup>19</sup> In this study, we focused on dissociation of butanol–propanol dimers, for which thermochemical properties are well-established<sup>20</sup> (see Table 1 for the summary of the literature thermochemical data). Furthermore, dissociation of protonated butanol–propanol dimers yields two monomer peaks of comparable intensities, which allows accurate and reproducible measurement of metastable peak shapes. The counter example of competing reactions with substantial entropy difference is given by fragmentation of protonated 1,2-ethylenediamine–pyrrolidine dimer. Protonation of diaminoalkanes is characterized by substantial negative entropy of protonation because these species dicoordinate the proton.<sup>21</sup> However, a recent study of proton affinities of diaminoalkanes carried out using the extended version of the kinetic method demonstrated that the kinetic method provides accurate PAs for these systems,<sup>22</sup> suggesting that dissociation of proton-bound dimers containing diamines is not associated with substantial reverse activation barriers, a necessary prerequisite for both the kinetic method and the approach based on KERD measurements previously proposed by us.<sup>5</sup>

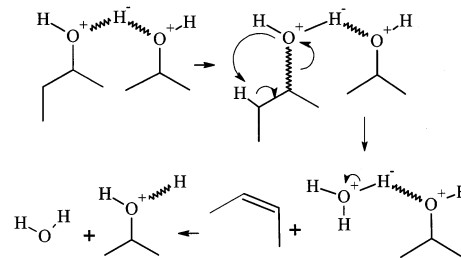
**1. Fragmentation of Butanol–Propanol Dimers.** Table 2 lists the average KERs and branching ratios for fragmentation of butanol–propanol dimers. Because of negligible differences in entropy effects for the formation of the two monomers, the branching ratios are solely determined by the difference in proton affinities of the two monomers (Table 1). It should be noted, however, that the value of the branching ratio for the 2-butanol–2-propanol dimer does not correspond to the reported large (>5 kcal/mol) difference in proton affinities of the two alcohols, which suggests that the literature value for the PA of 2-butanol is strongly overestimated.

**TABLE 2. Average KERs and Branching Ratios upon Fragmentation of Alcohol Dimers**

proton-bound dimer [B <sub>1</sub> -H <sup>+</sup> -B <sub>2</sub> ]	$\langle T \rangle$ (meV)		B <sub>1</sub> H <sup>+</sup> /B <sub>2</sub> H <sup>+</sup>
	61	75	
<i>n</i> -butanol- <i>n</i> -propanol	44	47	8.75 ± 0.04
<i>n</i> -butanol-2-propanol	65	58	0.225 ± 0.001
<i>i</i> -butanol- <i>n</i> -propanol	55	52	10.3 ± 0.3
<i>i</i> -butanol-2-propanol	61	45	0.200 ± 0.003
2-butanol-2-propanol	71	69	6.3 ± 0.1

Metastable peaks for the monomer fragments of the *n*-butanol-*n*-propanol dimer have pseudo-Gaussian shapes with average KERs of 44 and 47 meV for *n*-propanol and *n*-butanol, respectively. It was mentioned earlier that a larger KER should be observed for the monomer with higher proton affinity. Our result for the *n*-butanol-*n*-propanol dimer is in qualitative agreement with these expectations. However, most metastable peaks obtained from mixed dimers of primary and secondary alcohols are characterized by larger values of KERs. In many cases, the peaks are dish topped, indicative of high KER consistent with a reverse activation barrier. It therefore follows that branched alcohols represent a serious challenge for the kinetic method. Interestingly, the problem associated with these systems cannot be recognized based on the measurements of branching ratios alone. Because KER measurements are much more sensitive to detailed dynamics of dissociation, they should be used as a diagnostic tool for determining the presence of the reverse activation barrier.

*Mechanism of Dissociation of Alcohol Dimers.* It should be noted that Holmes et al. reported that the kinetic method was applicable only for primary alcohols.<sup>19</sup> These authors argued that for branched alcohols other fragmentation pathways such as loss of water or olefin elimination are dominant, indicating major structural rearrangements for the majority of protonated dimers. Relative intensities of the monomer peaks ( $m/z = 61$  and 75) and the peaks corresponding to the loss of water ( $m/z = 117$ ) and olefin elimination ( $m/z = 79$  and 93) from the protonated dimer observed in MIKEs spectra are listed in Table 3. Clearly, in all cases, the loss of water from the dimer is a major peak in the MIKEs spectra. For all dimers containing secondary alcohols, olefin elimination resulting in formation of either hydrated propanol or hydrated butanol becomes a dominant channel. Interestingly, in each case, only one of the two hydrated ions is produced in a large amount. It is important to note that the presence of competing dissociation pathways such as water or olefin loss does not prevent the application of the kinetic method to the formation of monomers. If the protonated monomers were formed from the dimers that did not rearrange prior to fragmentation, the branching ratio and the average KER would be determined only by the proton affinities of individual monomers and the kinetic method should be applicable. However, our KER measurements indicate that there is a major mechanistic difference between the formation of protonated monomers from dimers containing primary alcohols vs dimers containing secondary alcohols, resulting in

**SCHEME 1: Proposed Mechanism for Dissociation of Alcohol Dimers of Secondary Alcohols into Monomeric Species**

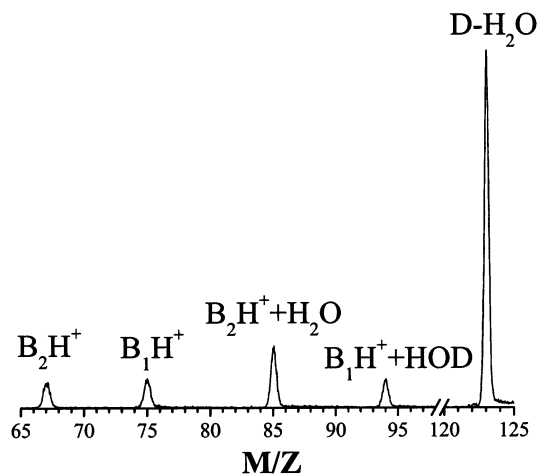
reverse activation barriers, which renders the kinetic method inapplicable for these systems.

The proposed mechanism is summarized in Scheme 1. Partial protonation of each monomer in the dimer ion results in weakening and cleavage of either C-O bond followed by the fast proton transfer from the protonated carbonium ion to the hydrated alcohol. The formation of the stable alkene is associated with a reverse activation barrier. Finally, the water molecule is eliminated from the hydrated alcohol resulting in the formation of the protonated monomer. Because of the lack of charge stabilization by the linear alkyl chain from the primary carbon, C-O bond cleavage is not likely to occur in primary alcohols. It is also less likely to occur for isobutanol as compared to 2-propanol or 2-butanol because in isobutanol a primary carbon atom is connected to the OH group. The proposed mechanism for monomer formation competes with the simple cleavage of the hydrogen bond leading to the same product ions. It rationalizes both the relative intensities of ions in the MIKEs spectra and the dishing of metastable peaks observed for secondary alcohols. For example, the only hydrated monomer observed for *n*-butanol-2-propanol, 2-butanol-*n*-propanol, and isobutanol-*n*-propanol dimers is the one containing the primary alcohol (Table 3). This is consistent with Scheme 1 because only the C-O bond of the secondary alcohol can be cleaved. The more significant stabilization of the charge in the carbonium ion is manifested by the preferential cleavage of the C-O bond of 2-propanol and the formation of hydrated isobutanol for the isobutanol-2-propanol pair and preferential formation of hydrated 2-propanol from the 2-butanol-2-propanol dimer.

Although loss of water is a major peak in MIKEs spectra, it does not interfere with the formation of protonated monomers. The mechanism for dehydration of alcohol dimers shown in Scheme 2 has been discussed previously for protonated methanol dimers.<sup>23</sup> It involves a backside nucleophilic attack from a neutral alcohol on the carbon adjacent to the OH group of the protonated alcohol with a water molecule as the leaving group (S<sub>N</sub>2 reaction). A similar mechanism was proposed for bimolecular alkylation of protonated alcohols, which has been studied in a great detail both experimentally<sup>24-27</sup> and theoretically.<sup>23,28,29</sup> Clearly, because this mechanism also involves the cleavage of C-O, a more facile water loss is observed for alcohols, in which the OH group is attached to the secondary carbon. The

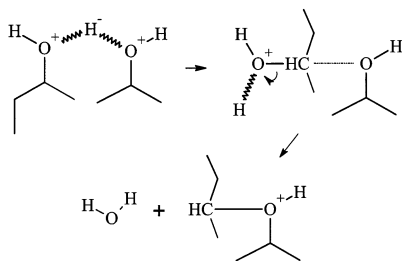
**TABLE 3: Relative Intensities of Peaks Observed in MIKEs Spectra of Alcohol Dimers**

proton-bound dimer [B <sub>1</sub> -H <sup>+</sup> -B <sub>2</sub> ]	B <sub>1</sub> H <sup>+</sup> $m/z$ 75	B <sub>1</sub> H <sup>+</sup> + H <sub>2</sub> O $m/z$ 93	B <sub>2</sub> H <sup>+</sup> $m/z$ 61	B <sub>2</sub> H <sup>+</sup> + H <sub>2</sub> O $m/z$ 79	[B <sub>1</sub> -H <sup>+</sup> -B <sub>2</sub> ] - H <sub>2</sub> O $m/z$ 117
<i>n</i> -butanol- <i>n</i> -propanol	51.4	1.2	12.4	5.5	29.5
<i>n</i> -butanol-2-propanol	1.4	10.6	4.0	0.0	84.0
2-butanol- <i>n</i> -propanol	10.7	0.0	0.4	31.3	57.6
2-butanol-2-propanol	5.5	0.9	0.8	31.6	61.2
isobutanol- <i>n</i> -propanol	43.4	1.7	5.5	26.3	23.1
isobutanol-2-propanol	1.8	15.0	6.9	1.3	75.0



**Figure 2.** MIKEs scan showing fragmentation of the isobutanol- $-(\text{CD}_3)_2\text{CHOH}$  dimer.

### SCHEME 2: Mechanism of Dehydration of Alcohols Dimers



dehydration of a protonated dimer results in the formation of stable protonated ether, which is not likely to dissociate into individual monomers.

We have also carried out MIKEs experiments involving dimers of butanol with partially deuterated 2-propanol,  $(\text{CD}_3)_2\text{CHOH}$ , to confirm or challenge the proposed mechanisms. Figure 2 shows an example of a MIKEs scan for the isobutanol- $(\text{CD}_3)_2\text{CHOH}$  dimer. The spectrum contains monomer peaks at  $m/z = 75$  and  $m/z = 67$  corresponding to the protonated isobutanol and protonated 1,1,1,3,3,3- $d_6$  2-propanol, respectively. We have not observed any hydrogen scrambling for all three butanol- $(\text{CD}_3)_2\text{CHOH}$  dimers. The dehydration product appears at  $m/z = 123$ , which corresponds to the loss of  $\text{H}_2\text{O}$  from the dimer. This observation is in good agreement with the mechanism shown in Scheme 2. The two hydrated monomer peaks appear at  $m/z = 94$ , corresponding to protonated isobutanol + HOD, and  $m/z = 85$ , corresponding to  $[(\text{CD}_3)_2\text{CHOH} + \text{H}_2\text{O}]\text{H}^+$ . Observation of the hydrated isobutanol peak at  $m/z = 94$  agrees with the mechanism shown in Scheme 1. According to Scheme 1, there is a proton transfer from the carbonium ion to the hydrated alcohol involving one of the hydrogens from a methyl group, which is fully deuterated in  $(\text{CD}_3)_2\text{CHOH}$ . Loss of HOD from the hydrated intermediate results in the formation of the isobutanol monomer at  $m/z = 75$ .

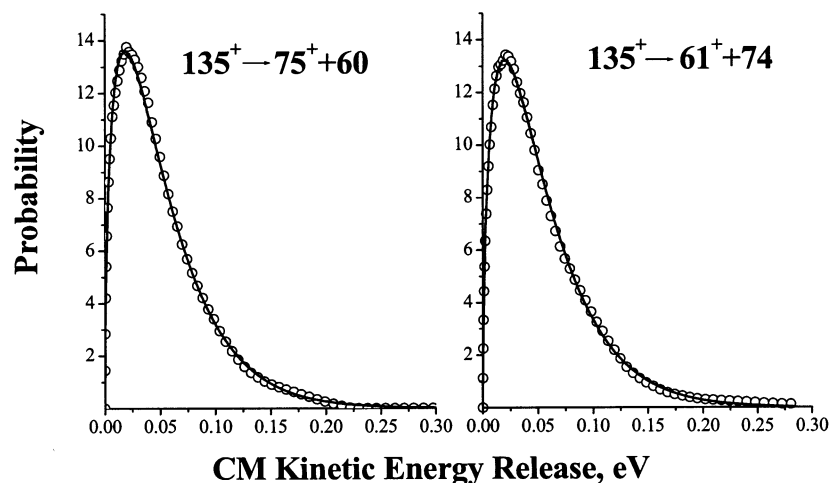
**Relative Proton Affinities and Reaction Entropies.** From the above discussion, it follows that the kinetic method can be applied only to the  $n$ -butanol- $n$ -propanol dimer, which fragments into two monomers via a simple cleavage of the hydrogen bond. Experimental KERDs together with the best fit using the function given by eq 9 are shown in Figure 3, and the modeling results are summarized in Table 4. The transition state temperature for the formation of protonated  $n$ -butanol,  $T_1^\ddagger$ , is somewhat higher than the transition state temperature for the formation of protonated  $n$ -propanol,  $T_2^\ddagger$ . This is an expected result because

of the higher proton affinity of  $n$ -butanol, which results in the lower dissociation threshold,  $\Delta E_1$ , for the formation of the corresponding protonated monomer and the higher transition state temperature,  $T_1^\ddagger$  (see Figure 1). It should be noted that different values of  $T_1^\ddagger$  and  $T_2^\ddagger$  were obtained depending on the source conditions with variations indicated by error bars. However, both temperatures shifted systematically from experiment to experiment with the difference between them remaining at  $20 \pm 7$  K. The entropy difference for the two reaction channels is very close to zero ( $\Delta(\Delta S^\ddagger) = -0.3 \pm 1.5$  cal/mol K). The large error bar originates from the variations in the relative values of transition state temperatures. However, in general, relative reaction entropies cannot be determined with greater precision than reported here.

The difference in dissociation thresholds,  $\Delta E_1 - \Delta E_2$ , is  $-1.0 \pm 0.3$  kcal/mol. This should be compared to  $\text{PA}(\text{B}_2) - \text{PA}(\text{B}_1)$  (see eq 8) for which ref 20 gives a value of  $-0.6$  kcal/mol. Adjusting the proton affinity of  $n$ -butanol to 189.7 kcal/mol as suggested by Holmes et al.<sup>19</sup> results in the difference in proton affinities of  $-1.7$  kcal/mol. Neither the original nor the adjusted experimental literature values fall within the 0.3 kcal/mol error bar obtained in this study. However, our relative proton affinity is rather close to the value suggested by Hunter and Lias.<sup>20</sup> Proton affinities of  $n$ -propanol and  $n$ -butanol calculated using a fairly high level of theory are 785.2 kJ/mol (187.7 kcal/mol) and 791.4 kJ/mol (189.1 kcal/mol),<sup>28</sup> respectively, with the relative proton affinity of  $-1.4$  kcal/mol being within 1 kcal/mol of the value determined in this study.

**2. Fragmentation of the Pyrrolidine-1,2-Ethylenediamine Dimer.** Dissociation of the pyrrolidine-ethylenediamine (Pyr-ED) dimer is characterized by very small average KERs: 26.5 meV for the protonated ethylenediamine and 24.5 meV for the protonated pyrrolidine. No other reaction channels were observed for this dimer. Similar to the  $n$ -butanol- $n$ -propanol dimer, the average KERs follow the proton affinities of monomeric species in the dimer. However, the branching ratio of 11.8 (Table 4) found for the Pyr-ED dimer favors the formation of the monomer with lower proton affinity, i.e., protonated pyrrolidine. This is a result of a significant entropy effect associated with protonation of ethylenediamine. Namely, because this molecule dicoordinates the proton, it is characterized by large negative entropy of protonation (Table 1). It follows that the formation of protonated ethylenediamine is strongly hindered because of the entropy effect, which results in the favored formation of protonated pyrrolidine from the Pyr-ED dimer.

Figure 4 represents typical KERDs for the Pyr-ED dimer fragmentation. Transition state temperatures derived from these distributions are listed in Table 4. Interestingly, these temperatures are significantly lower than the transition state temperatures for the  $n$ -butanol- $n$ -propanol dimer. Because the transition state temperature is higher for systems with deeper potential well and higher dissociation thresholds, this indicates that the latter is more strongly bound than the Pyr-ED dimer. The difference in the threshold energies for the two reaction channels determined from theoretical modeling is  $0.27 \pm 0.10$  kcal/mol, which is somewhat lower than the literature value for the relative proton affinities (0.8 kcal/mol).<sup>20</sup> The proton affinity of ethylenediamine determined using the extended version of the kinetic method is 226.6 kcal/mol,<sup>18</sup> which is equal to the proton affinity of pyrrolidine (Table 1), and suggests the relative proton affinity is equal to zero. A very similar value of 226.5 kcal/mol for the proton affinity of ethylenediamine was obtained using G2 calculations.<sup>29</sup> Cao et al. found a value of 226.8 kcal/

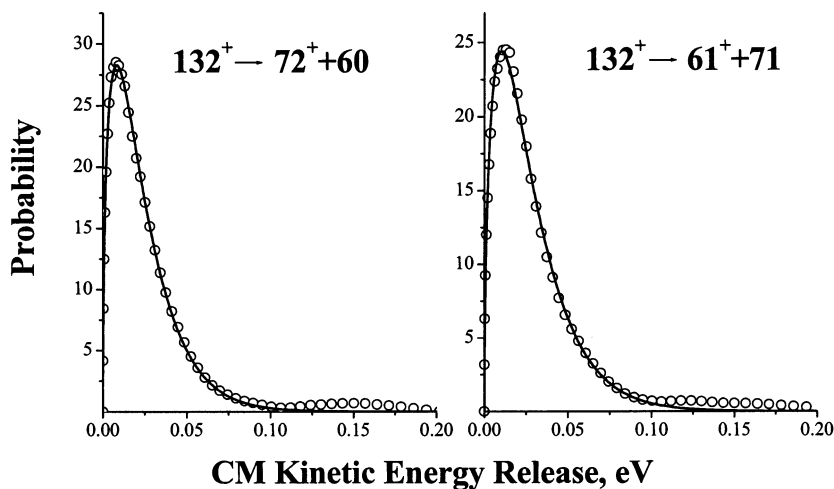


**Figure 3.** Experimental (open circles) and calculated (solid line) KERDs for dissociation of the *n*-butanol-*n*-propanol dimer ( $m/z = 135$ ); left panel shows KERD extracted from the peak at  $m/z = 75$  (protonated *n*-butanol); right panel shows KERD extracted from the peak at  $m/z = 61$  (protonated *n*-propanol).

**TABLE 4: Transition State Temperatures, Relative Dissociation Energies, and Relative Entropies for Reactions 1 and 2<sup>a</sup>**

$B_1 - H^+ - B_2$	BR <sup>b</sup>	$C^c$	$T_1^\ddagger$ (K)	$T_2^\ddagger$ (K)	$\Delta S_1^\ddagger - \Delta S_2^\ddagger$ <sup>d</sup>	$\Delta S_{p1} - \Delta S_{p2}$ <sup>e</sup>	$\Delta E_1 - \Delta E_2$ <sup>f</sup>	$PA_2 - PA_1$ <sup>g</sup>
<i>n</i> -butanol- <i>n</i> -propanol	$8.7 \pm 0.1$	42	$404 \pm 10$	$387 \pm 10$	$-0.3 \pm 1.5$	0	$-1.0 \pm 0.3$	-0.6
pyrrolidine-1,2-ethylenediamine	$11.8 \pm 0.2$	29	$200 \pm 10$	$212 \pm 10$	$8.2 \pm 0.5$	5	$0.27 \pm 0.10$	0.8

<sup>a</sup> Italicized is the monomer with lower proton affinity. <sup>b</sup> branching ratio,  $B_1H^+/B_2H^+$ ; <sup>c</sup> dimensionless heat capacity; <sup>d</sup> the difference in reaction entropies for reactions 1 and 2 in cal/mol K; <sup>e</sup> the difference in protonation entropies from ref 20 in cal/mol K; <sup>f</sup> the difference in threshold energies for reactions 1 and 2 in kcal/mol; <sup>g</sup> the difference in proton affinities of  $B_2$  and  $B_1$  in kcal/mol (ref 20).



**Figure 4.** Experimental (open circles) and calculated (solid line) KERDs for dissociation of the pyrrolidine-1,2-ethylenediamine dimer ( $m/z = 132$ ); left panel shows KERD extracted from the peak at  $m/z = 72$  (protonated pyrrolidine); right panel shows KERD extracted from the peak at  $m/z = 61$  (protonated ethylenediamine).

mol (949 kJ/mol) for the proton affinity of ethylenediamine using the kinetic method.<sup>30</sup> The relative proton affinity then equals to 0.2 kcal/mol, which is in excellent agreement with our data.

The difference in reaction entropies,  $\Delta(\Delta S^\ddagger)$ , of  $8.2 \pm 0.5$  cal/mol K is higher than the difference in protonation entropies,  $\Delta(\Delta S_p)$ , of 5 cal/mol K listed in ref 20. An even lower  $\Delta(\Delta S_p)$  can be derived from theoretical calculations, which established a value of  $-4$  cal/mol K for the protonation entropy of ethylenediamine.<sup>31</sup> The experimental data for  $\Delta(\Delta S_p)$  obtained using the equilibrium method is rather scattered with the  $\Delta(\Delta S_p)$  of 5.8 cal/mol K found by Meot-Ner et al.<sup>21</sup> and  $\Delta(\Delta S_p)$  of 12.7 cal/mol K reported by Yamdagni and Kebarle.<sup>33</sup> Comparison of experimental and calculated thermochemical properties for a series of relatively small molecules demonstrated a fairly large variation between the experimental and the

theoretical entropies of protonation, while a better agreement was found for gas phase basicities and proton affinities.<sup>34</sup>

It follows that experimentally determined protonation entropies are characterized by large uncertainties. The difference in reaction entropies determined in this study equals the entropy difference between the transition states for reactions 1 and 2 resulting in formation of monomers, while  $\Delta(\Delta S_p) = S(B_1H^+) - S(B_1) - S(B_2H^+) + S(B_2)$ . The difference in reaction entropies is close to the difference in protonation entropies only when the transition states for both reactions have very similar vibrational and rotational characteristics to the two separated products. However, if the transition state is located relatively far away from the products,  $\Delta(\Delta S^\ddagger)$  and  $\Delta(\Delta S_p)$  could be significantly different. Theoretical calculations demonstrated that protonation of ethylenediamine results in a significant increase in rotational barriers around the carbon-carbon bond and the

bond between one of the carbon atoms and the NH<sub>2</sub> group.<sup>31</sup> The length of the hydrogen bond in the protonated species is 1.89 Å. It is reasonable to assume that ethylenediamine has a similar structure in the dimer. However, lengthening of the hydrogen bond in the transition state for dimer dissociation could result in significant reduction in rotational barriers within ethylenediamine and a significant increase in reaction entropy in comparison with both the reactant and the products.

## Conclusions

In this work, we evaluated a new method for determining relative proton affinities and relative reaction entropies for dissociation of proton-bound dimers. The method is based on simultaneous measurement of KERDs and the branching ratio for two competing reactions followed by extracting thermochemical information using FHBT. The first application of the KERD measurements for thermochemical determinations demonstrated both success and challenges associated with kinetic measurements even for very simple systems such as secondary alcohols. We found that the proposed approach offers several unique advantages over the existing versions of the kinetic method:

(i) The relative proton affinity of the unknown can be extracted from a relative measurement vs a single reference base. This eliminates major complications associated with choosing a series of reference bases with known proton affinities, as required in the kinetic method.

(ii) Because KERDs are very sensitive to the details of the potential energy surface, measurement of KERDs can be used as a diagnostic tool for the intelligent choice of reference bases. For example, we found that the kinetic method could not be applied to 2-butanol and isobutanol because of the presence of an alternative fragmentation pathway resulting in the formation of monomers characterized by a reverse activation barrier. This conclusion could not be reached by measuring branching ratios for competing reactions. KERD measurement also revealed that there is no reverse activation barrier associated with fragmentation of the pyrrolidine–ethylenediamine dimer.

(iii) In the proposed approach, the relative proton affinities are extracted directly from the relative widths of metastable peaks; these can be determined fairly accurately provided the instrument is properly calibrated for KERD measurements. The relative proton affinities obtained in this study are in a good agreement with literature data, and the error bars on the relative values are fairly small. In contrast, the kinetic method relies on the measurement of relative gas phase basicities and the relative proton affinities are extracted indirectly from the experimental data. As a result, the accuracy of proton affinity determinations using the kinetic method depends on the accuracy with which the relative entropies are determined.

(iv) Our approach uses the branching ratio between the protonated monomers and the independent measurement of relative energetics of the two reactions to obtain the difference in reaction entropies. We found that for the *n*-butanol–*n*-propanol dimer the values of  $\Delta(\Delta S^\ddagger)$  and  $\Delta(\Delta S_p)$  are very close. However, this is not the case for the pyrrolidine–ethylenediamine dimer, for which  $\Delta(\Delta S^\ddagger)$  is higher than  $\Delta(\Delta S_p)$ .

In summary, the proposed approach can be utilized both for relative thermochemical determinations and for studies of the dynamics of dissociation of weakly bound complexes and the relative energetics of noncovalent interactions.

**Acknowledgment.** All of the work described herein was conducted at the W. R. Wiley Environmental Molecular

Sciences Laboratory (EMSL), a national scientific user facility sponsored by the U.S. Department of Energy and located at Pacific Northwest National Laboratory. PNNL is operated by Battelle for the U.S. Department of Energy. Research at EMSL was carried out within the project 40457 supported by the Office of Basic Energy Sciences of the U.S. Department of Energy. One of us (J.J.H.) was supported by an ERULF fellowship, which is gratefully acknowledged. We are thankful to Dr. Robert H. Bateman for a very helpful discussion on the instrument modifications for accurate KERD measurements and Dr. Paul Mayer for a very helpful discussion on the structures of alcohol dimers. We are also thankful to Drs. Chris Rodriguez and Michael Siu for providing us with vibrational frequencies of protonated diamines.

## References and Notes

- (1) Cooks, R. G.; Kruger, T. L. *J. Am. Chem. Soc.* **1977**, *99*, 1279.
- (2) McLuckey, S. A.; Cameron, D.; Cooks, R. G. *J. Am. Chem. Soc.* **1981**, *103*, 1313.
- (3) Klots, C. E. *J. Chem. Phys.* **1989**, *90*, 4470.
- (4) Klots, C. E. In *Unimolecular and Bimolecular Reaction Dynamics*; Ng, C. Y., Baer, T., Powis, I., Eds.; John Wiley & Sons Ltd.: New York, 1994.
- (5) Laskin, J.; Futrell, J. H. *J. Phys. Chem. A* **2000**, *104*, 8829.
- (6) Cheng, X.; Wu, Z.; Fenselau, C. *J. Am. Chem. Soc.* **1993**, *115*, 4844.
- (7) Zheng, X.; Cooks, R. G. 50th ASMS Conference on Mass Spectrometry and Allied Topics, Orlando, FL, 2002.
- (8) Laskin, J.; Lifshitz, C. *J. Mass Spectrom.* **2001**, *36*, 459.
- (9) Klots, C. E. *Z. Phys. D* **1991**, *21*, 335.
- (10) Sandler, P.; Peres, T.; Weissman, G.; Lifshitz, C. *Ber. Bunsen-Ges. Phys. Chem.* **1992**, *96*, 1195.
- (11) Laskin, J.; Peres, T.; Khong, A.; Jiménez-Vázquez, H. A.; Cross, R. J.; Saunders, M.; Bethune, D. S.; de Vries, M. S.; Lifshitz, C. *Int. J. Mass Spectrom. Ion Processes* **1999**, *187*, 61.
- (12) Porter, C. J.; Brenton, A. G.; Beynon, J. H. *Int. J. Mass Spectrom. Ion Phys.* **1980**, *35*, 353.
- (13) Proctor, C. J.; Porter, C. J.; Brenton, A. G.; Beynon, J. H. *Int. J. Mass Spectrom. Ion Phys.* **1981**, *39*, 9.
- (14) Boyd, R. K.; Kingston, E. E.; Brenton, A. G.; Beynon, J. H. *Proc. R. Soc. London A* **1984**, *392*, 59.
- (15) Jones, E. G.; Bauman, L. E.; Beynon, J. H.; Cooks, R. G. *Org. Mass Spectrom.* **1973**, *7*, 185.
- (16) McCormack, J. A. D.; Mayer, P. M. *Int. J. Mass Spectrom.* **2001**, *207*, 183.
- (17) El-Gorary, T. M.; Soliman, M. S. *Spectrochim. Acta A* **2001**, *57*, 2647.
- (18) Rodriguez, C. F.; Siu, K. W. M. Private communication.
- (19) Holmes, J. L.; Aurby, C.; Mayer, P. M. *J. Phys. Chem. A* **1999**, *103*, 705.
- (20) Hunter, E. P. L.; Lias, S. G. *J. Phys. Chem. Ref. Data* **1998**, *27*, 413.
- (21) Meot-Ner (Mautner), M.; Hamlet, P.; Hunter, E. P.; Field, F. H. *J. Am. Chem. Soc.* **1980**, *102*, 6393.
- (22) Wang, Z.; Chu, I. K.; Rodriguez, C. F.; Hopkinson, A. C.; Siu, K. W. M. *J. Phys. Chem. A* **1999**, *103*, 8700.
- (23) Bouchoux, G.; Choret, N. *Rapid Commun. Mass Spectrom.* **1997**, *11*, 1799.
- (24) Beauchamp, J. L.; Caserio, M. C. *J. Am. Chem. Soc.* **1972**, *94*, 2638.
- (25) Hall, D. G.; Gupta, C.; Morton, T. H. *J. Am. Chem. Soc.* **1981**, *103*, 2416.
- (26) Kleingeld, J. C.; Nibbering, N. M. M. *Org. Mass Spectrom.* **1982**, *17*, 136.
- (27) Karpas, Z.; Meot-Ner (Mautner), M. *J. Phys. Chem.* **1989**, *93*, 1859.
- (28) Raghavachari, K.; Chandrasekhar, J.; Burnier, R. C. *J. Am. Chem. Soc.* **1984**, *106*, 3124.
- (29) Sheldon, J. C.; Currie, G. J.; Bowie, J. H. *J. Chem. Soc., Perkin Trans. 2* **1986** 941.
- (30) Ligon, A. P. *J. Phys. Chem. A* **2000**, *104*, 8739.
- (31) Bouchoux, G.; Choret, N.; Berruyer-Penaud, F. *J. Phys. Chem. A* **2001**, *105*, 3989.
- (32) Cao, J.; Aurby, C.; Holmes, J. L. *J. Phys. Chem. A* **2000**, *104*, 10045.
- (33) Yamdagni, R.; Kebarle, P. *J. Am. Chem. Soc.* **1973**, *95*, 3504.
- (34) East, A. L. L.; Smith, B. J.; Radom, L. *J. Am. Chem. Soc.* **1997**, *119*, 9014.